Journal Name

ARTICLE

Site-selective reversible Diels-Alder reaction between a biphenylene-based polyarene and a semiconductor surface

Received 00th January 20xx,
Accepted 00th January 20xx

DOI: 10.1039/x0xx00000x

www.rsc.org/

Szymon Godlewski,‡*[,a] Mads Engelund,‡[b] Diego Peña,[c] Rafał Zuzak,[a] Hiroyo Kawai,*[,d] Marek Kolmer,[a] Jorge Caeiro,[c] Enrique Guitián,[c] K. Peter C. Vollhardt,[e] Daniel Sánchez-Portal,[b] Marek Szymonski[a] and Dolores Pérez*[,c]

Understanding the mechanisms involved in the covalent attachment of organic molecules to surfaces is a major challenge for nanotechnology and surface science. On the basis of classical organic chemistry mechanistic considerations, key issues such as selectivity and reactivity of the organic adsorbates could be rationalized and exploited for the design of molecular-scale circuits and devices. Here we use tris(benzocyclobutadieno)triphenylene, a singular Y-shaped hydrocarbon containing antiaromatic cyclobutadienoid rings, as a molecular probe to study the reaction of polycyclic conjugated molecules with atomic scale moieties, dangling-bond (DB) dimers on a hydrogen-passivated Ge(001):H surface. By combining molecular design, synthesis, scanning tunneling microscopy and spectroscopy (STM/STS) and computational modeling, we show that the attachment involves a concerted [4+2] cycloaddition reaction that is completely site-selective and fully reversible. This selectivity, governed by the bond alternation induced by the presence of the cyclobutadienoid rings, allows for the control of the orientation of the molecules with respect to the surface DB-patterning. We also demonstrate that by judicious modification of the electronic levels of the polycyclic benzenoid through substituents, the reaction barrier height can be modified. Finally, we show that after deliberate tip-induced covalent bond cleavage, adsorbed molecules can be used to fine tune the electronic states of the DB dimer. This power to engineer deliberately the bonding configuration and electronic properties opens new perspectives for creating prototypical nanoscale circuitry.

Introduction

Controlling chemical reactions of organic molecules on surfaces is attracting growing attention, driven both by potential applications in the construction of future nanoscale devices and by a fundamental interest in the basic processes leading to tailored bond formation and cleavage between molecules and surface reactive sites.[1] Recent developments in scanning tunnelling microscopy (STM) and atomic force microscopy (AFM) have propelled advances in imaging of reactants and products with atomic or sub-molecular resolution.[2] But as important as the physical evidences of the chemisorption of organic molecules on surfaces is the understanding of the mechanisms of such reactions in terms of fundamental chemistry concepts.[3] In fact, the possibility of applying the rationale of organic chemistry to surface functionalization could provide invaluable insights for the design of molecules that can attach to the surface in a specific manner and orientation.

The surfaces of semiconductors are ideal candidates for the study of reactions with organic molecules.[4] Among the different possible substrates, functionalized silicon and germanium (001) surfaces[5] have attracted strong attention due to their leading role in the microelectronic industry. Numerous examples of molecules forming covalent bonds with silicon and germanium surfaces have been reported, showing both local modifications of the conformation, bond formation and cleavage, as well as long-range phenomena and non-local interactions.[6] Analogies between many of these bond-forming processes and classical organic chemistry reactions have been established, with the surface acting as a molecular reagent.[5d]

The functionalization of hydrogen passivated Si or Ge surfaces containing atomic scale defects – unsaturated dangling bonds (DBs),[7] or even DB structures created intentionally by H atom extraction[8] – provides additional opportunities for the construction of prototypical molecular scale devices. It has

[a] Centre for Nanometer-Scale Science and Advanced Materials, NANOSAM, Faculty of Physics, Astronomy and Applied Computer Science, Jagiellonian University, Lojasiewicza 11, PL 30-348 Krakow, Poland. E-mail: szymon.godlewski@uj.edu.pl
[b] Centro de Física de Materiales CSIC-UPV/EHU and DIPC, Paseo Manuel de Lardizabal 5, E-20018, Donostia-San Sebastián, Spain.
[c] Centro Singular de Investigación en Química Biolóxica e Materiais Moleculares (CIQUS) and Departamento de Química Orgánica, Universidade de Santiago de Compostela, 15782 Santiago de Compostela, Spain. E-mail: dolores.perez@usc.es
[d] Institute of Materials Research and Engineering, 2 Fusionopolis Way, Innovis, #08-03, Singapore 138634. E-mail: kawaih@imre.a-star.edu.sg
[e] Department of Chemistry, University of California at Berkeley, Berkeley, CA 94720-1460, USA.

† Electronic supplementary information (ESI) available: Synthesis and characterization data. Details of calculations.. Results with hexakis(hexyloxy)-substituted derivative. Structures of molecules with EHMO calculated molecular orbitals. Additional STM images. Attachment path and electronic properties for the hexafluorotribiphenylene derivative.. Properties of molecules physisorbed on a dangling bond dimer. Interaction of tribiphenylenes with single dangling bonds. See DOI: xxxxxxx

‡ These authors contributed equally.

been demonstrated that single DBs can anchor organic compounds by forming covalent bonds[9] or through weak van der Waals interactions[10] and, interestingly, that the charge state of the DBs can influence significantly the molecule's behavior.[9,11] Furthermore, compounds with conjugated π-system can react with Ge or Si surface DB dimers giving rise to different bonding configurations, including those associated with formal [2+2] and [4+2] (Diels-Alder) cycloadditions.[4,12] The mechanisms behind such transformations, through either concerted or diradical stepwise pathways, are dependent on the particular semiconductor surface.[13] Covalent functionalization with aromatic molecules has been limited primarily to relatively small molecular entities,[14] although the chemical attachment of some polycyclic aromatic hydrocarbons (PAHs), postulated as potential components of molecular electronic devices, has also been explored.[15] Previously, some of us investigated single, three-fold symmetric, Y-shaped trinaphthylene ([7]starphene, **1**),[16] recently proposed as a molecular rotational switch on hydrogen terminated Ge(001):H[17] and as a single-molecule logic gate on Au(111)[18] surfaces. The geometries observed for the adsorption of **1** on germanium DB dimers are consistent with a formal [4+2] cycloaddition of this molecule with the paired DBs.

Among the different families of polycyclic conjugated hydrocarbons of interest in molecular electronics, those combining fused four-membered cyclobutadienoid and six-membered benzenoid rings are particularly intriguing, because of the unique properties associated with the alternating antiaromatic and aromatic circuits.[20] Both experimental and theoretical studies show that the six-membered benzenoid rings in these molecules display significant bond alternation,[21] a feature that determines their reactivity. Besides the linear, angular and triangular [N]phenylenes[22] and phenylene-containing acenes,[23] phenes and starphenes,[24] isomeric graphene nanostructures containing fused biphenylene moieties have recently received significant attention.[25] However, to the best of our knowledge there are no reports on the covalent functionalization of semiconductor surfaces with biphenylene-containing PAHs.

Herein we describe the study of molecules with the tris(benzocyclobutadieno)triphenylene core **2** (hereafter referred to as tribiphenylenes) on the Ge(001):H surface. The three-fold symmetric geometry of **2a**[24] is closely related to that of trinaphthylene **1**[26] (see Figure 1), but the presence of the antiaromatic cyclobutadienoid rings in **2a** induces bond alternation in the fused benzene rings, thus fixing the position of the possible diene-like functionalities that could participate in a hypothetical [4+2] cycloaddition with DB dimers on the passivated germanium surface. We decided to exploit this structural feature to address some fundamental issues in surface functionalization, focusing on unveiling the mechanism of the chemisorption reaction and controlling the attachment architecture. Our hypothesis is that a concerted, orbital symmetry governed Diels-Alder reaction should be site selective, promoting the binding of **2a** in a particular

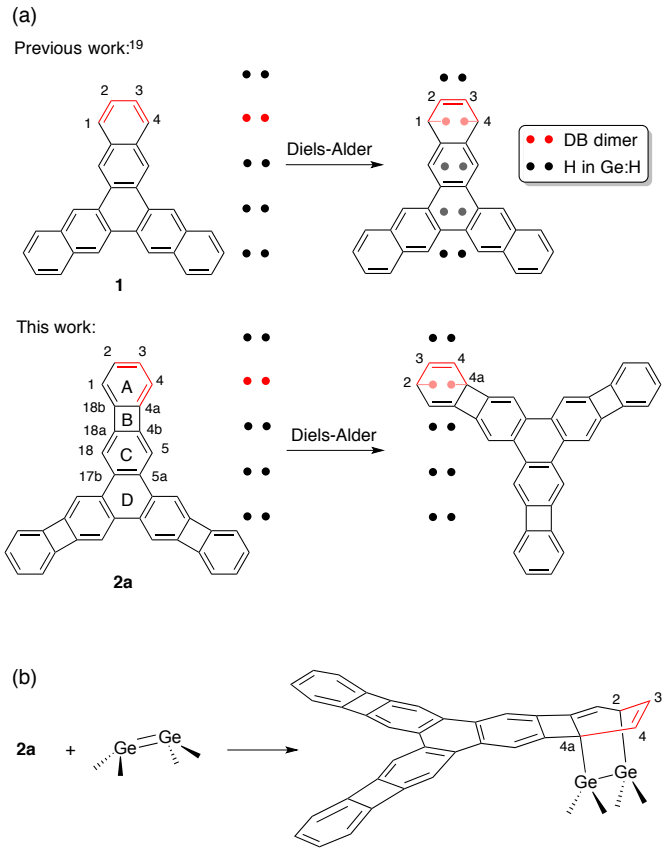

Figure 1 (a) Representative resonance structures of trinaphthylene **1**, tribiphenylene **2a** and sketch of the expected Diels-Alder reaction with DB dimers on the Ge(001):H surface; the location of diene-like functionalities in one of the arms of each molecule is drawn in red. (b) Schematic representation of the expected reaction of **2a** with a Ge(001) DB dimer.

orientation with respect to the DB dimer rows, and giving rise to binding patterns different from those observed for the analogous trinaphthylene (**1**) (Figure 1). Our detailed STM simulations and computation of the trajectory of the attachment, which shows no intermediate species, provides strong evidence for a site selective, concerted [4+2] Diels-Alder mechanism between these star-shaped PAHs and the DB-dimers on the passivated germanium surface. Moreover, our study highlights the feasibility of using molecular design to control not only the architecture of the attachment, but also the binding energy and the reaction barrier.

Results and discussion

Synthesis and characterization of tribiphenylenes 2a–c. The synthesis of tribiphenylene **2a** and the substituted derivatives **2b** and **2c**, containing electron-withdrawing and electron-donating groups, respectively, is shown in Scheme 1. First, the assembly of the biphenylene core was achieved by cobalt-catalysed [2+2+2] cycloaddition of the corresponding 1,2-diethynylarenes **3a–c** with bis(trimethylsilyl)acetylene (BTMSA). Functional group manipulation allowed the transformation of **4a–c** into the *o*-(trimethylsilyl)aryl triflates **5a–c**, which upon treatment with fluoride in the presence of

catalytic $Pd(PPh_3)_4$ afforded the corresponding tribiphenylenes **2a–c**, as a result of the palladium-catalysed cyclotrimerization of arynes **6**.[24,27] While **2a** and **2b** are highly insoluble in common solvents, the peripheral hexyloxy chains in **2c** increased solubility dramatically, allowing full spectroscopic characterization of this compound. The experimental HOMO-LUMO gaps for **2a–c**, determined from the UV/Vis spectra and cyclic voltammetry measurements (see ESI†, Section 3) are in agreement with the theoretically calculated values of around 3 eV.

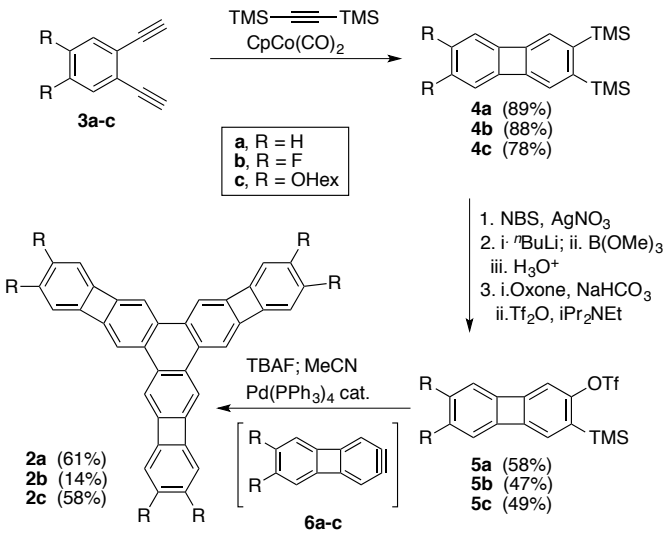

Scheme 1 Synthesis of tribiphenylenes **2a-c.** See ESI† for experimental details.

We have reported previously that both the aromaticity parameters and the calculated bond distances for **2a** imply a significant degree of bond localization, and thus reduced diatropism, in rings C and A[24] (see Figure 1). On the basis of these findings and the known selectivity trends for [4+2] cycloadditions of some phenylenes,[28] we predict that a Diels-Alder reaction of tribiphenylenes **2** should involve the diene moiety C(2)–C(4a) depicted in red in Figure 1. Preliminary calculations of the stability of the different possible cycloadducts of **2a** with a hypothetical Ge–Ge double bond also support this assumption (see ESI†, Section 4 for details).

Tribiphenylene molecules on the Ge(001):H surface. As discussed in detail in our previous studies, the Ge(001):H surface contains two major defect types, i.e., single hydrogen vacancies (dangling bonds, DBs) and dangling bond dimers (DB dimers).[8,9a] These defects may interact with a variety of structures,[10–12,16,17] and recently it was shown that a small fraction of planar starphene molecules **1** were adsorbed by weak van der Waals interactions on single DBs,[11] while the vast majority was covalently bonded to DB dimers in two different bonding configurations,[19] although the details of the reaction remained unexplored. Here, after deposition of tribiphenylene **2a** on the surface, all the adsorbed molecules of **2a** are found in an identical configuration, with one molecule branch oriented along surface reconstruction rows, as indicated by white circles in Figure 2a,b, but in contrast to trinaphthylene **1**,[19] tribiphenylene **2a** is located asymmetrically over the rows, as the arm parallel to surface rows is certainly not forming a bond with the surface DB dimer. Thus, there is a striking difference in the interaction of the two molecules with the surface atomic scale defects, as we had predicted on the basis of simple structural and mechanistic considerations (see Figure 1).

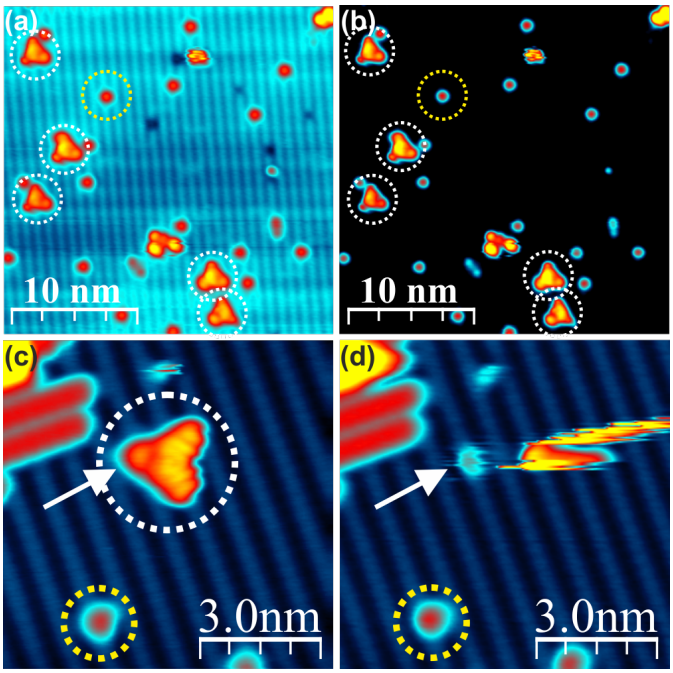

Figure 2. Filled state STM images of tribiphenylene **2a** on a Ge(001):H surface. Images (a) and (b) show the same area with the image contrast adjusted to surface rows and molecules, respectively. Images (c) and (d) show the same area, before and after molecule removal from the DB dimer, respectively. The molecules located on the surface DB dimers are marked with white dashed circles, those one surface single DBs are highlighted with a yellow dashed circle, white arrows in (c) and (d) indicate the location of the DB dimer. Scanning parameters: tunnelling current: 10 pA (a, b), 5 pA (c, d); bias voltage: –2.0 V (all panels).

The adsorption site can be clearly identified when the molecule is displaced from its initial position during STM imaging, as shown in Figure 2c,d. The manipulation event shows that the molecule is initially located over a DB dimer. After molecule removal, the DB dimer exhibits a streaky pattern due to rapid oscillations induced by tunnelling electrons[8a,b] between the two equivalent tilted equilibrium configurations of the dimer. The comparison of STM images acquired before (Figure 2c) and after (Figure 2d) molecule removal shows that the molecule located over the DB dimer exhibits a different appearance of the arm centred directly over the DB dimer site compared to the two remaining arms placed over the hydrogenated surface. It is important to note that when a sufficient amount of **2a** is deposited, all DB dimers are covered by tribiphenylene molecules with identical orientation.

To analyse the interaction of the molecule with the atomic scale defects, we have performed density functional theory (DFT) modelling, starting from several initial geometries. The most stable configuration is achieved for the molecule forming two covalent bonds with the DB dimer as shown in Figure 3e, characterized by a binding energy of 2.15 eV. During attachment, the outer benzene ring bends and forms two covalent bonds with both Ge atoms of the DB dimer, which becomes unbuckled. The attachment also requires deformation of the initially planar molecular structure. To establish agreement of the calculated molecular configuration with experiment, we have performed STM image computations based on Green's function modelling of the whole tunnelling junction.[16,17,29] The experimentally observed STM topography shown in Figure 3a is in close agreement with the calculated STM of a molecule covalently bonded to the DB dimer, shown in Figure 3b.

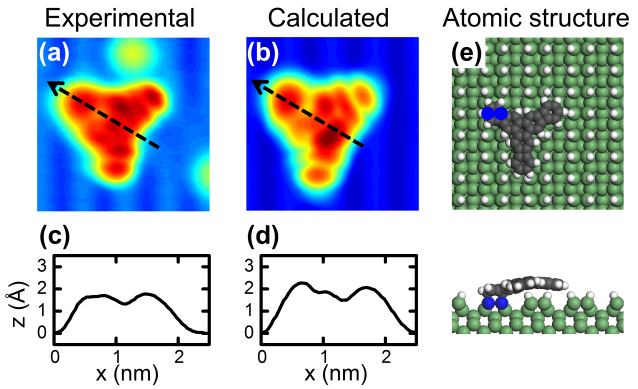

Figure 3. Tribiphenylene **2a** covalently attached to the surface DB dimer on a Ge(001):H surface. (a) Filled state STM image, tunnelling current: 2 pA; bias voltage: –2.0 V; (b) calculated STM topography, tunnelling current: 2 pA; bias voltage: –1.2V; (c) and (d) cross sections over the experimental and calculated images, respectively; (e) structural image.

Remarkably, our results demonstrate that the chemisorption reaction of **2a** is completely site-selective, i.e., there are no molecules attached to surface DB dimers in any other configuration, affording bonding through positions C(2) and C(4a) [or the equivalent C(3)–C(18a) diene], in contrast to the preferential 1,4-attachment observed for trinaphthylene (**1**)[19] (see Figure 1). The experimentally observed and theoretically predicted most stable configuration is fully consistent with a concerted Diels-Alder mechanism for the attachment reaction, in which the molecule plays the role of a conjugated diene [C(2)–C(4a)], while the surface DB dimer acts as the dienophile. The site selectivity can be understood on the basis of the considerations disclosed above. It is worth noting that cycloaddition through other possible diene sites in **2a** [C(1)–C(4) or C(6)–C(18), see Figure 1] would lead to unfavourable benzocyclobutadiene substructures. Thus, we should emphasize that by introduction of the four-membered rings in the molecular design, we can selectively control the orientation of the molecule bonding with the surface DB dimer.

We analyse here in more detail the bond formation between the molecule and the surface DB dimer. For this purpose, we have applied the Nudged-Elastic-Band (NEB) method[30] to investigate the adsorption/desorption path of the tribiphenylene molecule attached to the DB dimer site, which is visualized in Figure 4 displaying the molecule configurations with the calculated energies. In this approach, we studied the path from the attached configuration (geometry number 13 on the right, Figure 4) to the physisorbed state located nearby on a hydrogenated Ge(001):H surface (geometry number 1 on the left, Figure 4). The diagram shows that the attachment proceeds through a transition state with a calculated energy barrier of approximately 0.64 eV (1.28 eV for molecule detachment) with no additional intermediate states. This lack of intermediates points to a concerted reaction – consistent with a Diels-Alder [4+2] cycloaddition mechanism – with both Ge–C bonds being formed in a single step.

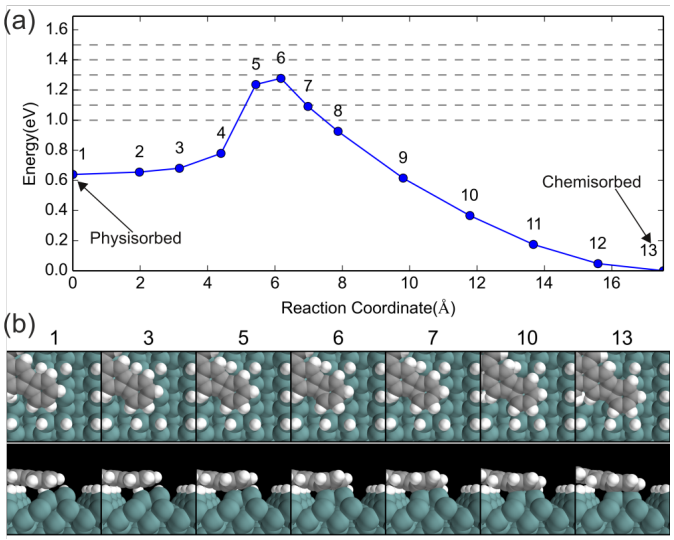

Figure 4. (a) Calculated attachment path of tribiphenylene **2a** to a DB dimer. The energies are plotted against a collective reaction coordinate (see ESI†, Figure S19). (b) Selected configurations of the molecule on the attachment path.

The introduction of substituents, which could potentially modulate the reactivity and/or the electronic properties of molecules on semiconductor surfaces, is an important issue for the future design of functional molecular devices. Thus, we explored the behaviour of substituted tribiphenylenes **2b** and **2c** deposited on Ge(001):H surface. While the adsorption of hexakis(hexyloxy)-substituted derivative **2c** resulted in multiple bonding configurations, probably due to steric interactions induced by the peripheral functionalization (see Figure S5 in ESI†), the hexafluoro derivative **2b** showed similar reactivity and the same site-selectivity as the parent tribiphenylene **2a** with a slightly lower binding energy of 1.93 eV (Figure 5 and Figure S20 in ESI†). The NEB calculations of the adsorption/desorption path support, similar to the parent species, a concerted mechanism with no intermediate species with a slightly higher energy barrier reaching 0.82 eV (1.37 eV for molecule escape, see Figure S19 in ESI†), which is in

agreement with the slight decrease of the HOMO energy for the hexafluorotribiphenylene (see Figures S21, S22 in ESI†).

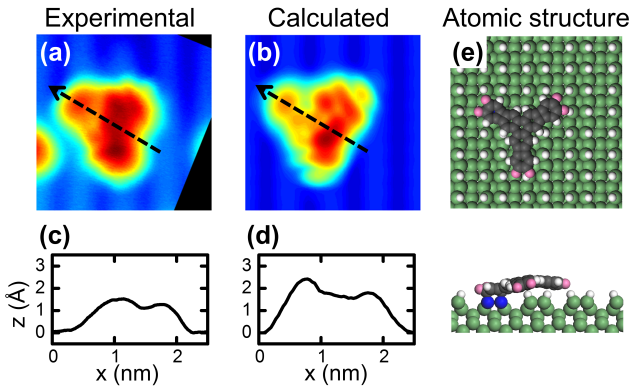

Figure 5. Hexafluorotribiphenylene **2b** covalently attached to the surface DB dimer on Ge(001):H. (a) Filled state STM image, tunnelling current: 10 pA; bias voltage: –2.0 V; (b) calculated STM topography, tunnelling current: 10 pA; bias voltage: –1.2 V; (c) and (d) cross sections over the experimental and calculated images, respectively; (e) structural image.

Reversible covalent attachment. It is interesting to note that the covalent bonds between the tribiphenylene molecule and the DB dimer can be reversibly cleaved and restored by means of the STM tip. Moreover, when the bonds are cleaved, through a process which can be understood as a retro-Diels-Alder reaction, the molecule may still stay located over a DB dimer, as illustrated in Figure 6.

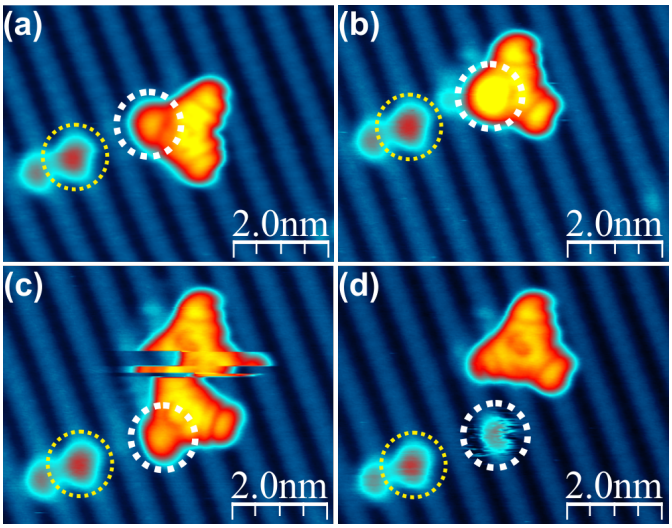

Figure 6. Filled state STM images illustrating reversible chemisorption between a tribiphenylene **2a** and a DB dimer: (a) The molecule covalently bonded to the DB dimer; (b) the molecule still located over the DB dimer after bond cleavage; (c) the molecule again chemically attached to the DB dimer; the streaky pattern in the upper part of the image originates from the movements of the molecule after subsequent bond cleavage; (d) the molecule located on fully hydrogenated Ge(001):H surface with clearly visible streaky pattern of the oscillating bare DB dimer; the white dashed circle marks the position of the DB dimer, the yellow circle indicates the surface defect used as a position marker. All images were acquired with tunnelling current 2 pA and bias voltage –2.0 V.

Initially the molecule is chemically attached to the DB dimer (Figure 6a). Then, by application of a positive voltage pulse (+3.0 V) electrons are injected and the bonds are cleaved, although the molecule still stays located over the DB dimer (Figure 6b). In this configuration one branch of the molecule points in the direction perpendicular to the surface reconstructed rows. Further, by application of a subsequent voltage pulse, the bonds between the molecule and the DB dimer are recreated, and the molecule is found again in the chemisorbed configuration, as documented in Figure 6c. The streaky pattern observed in the upper part of the image originates from unintentional removal of the molecule from the DB dimer during STM imaging, giving rise to the final configuration shown in Fig. 6d, where the molecule appears physisorbed in a fully H-saturated area away from the DB-dimer. At this point it is important to note that although the covalently bonded configuration is expected to be the most energetically favoured, as supported by the results described above (configuration of the molecules after deposition) and by calculations (see Figures S12-S14 in ESI†), the STM manipulation described in Figure 6 is performed at liquid helium temperature, thus the system is frozen and has not enough energy to go back to the most stable configuration spontaneously after bond cleavage. Therefore, both configurations, i.e., that with covalent bonds and that physisorbed over buckled DB dimers are observed with STM.

Electronic properties. To analyse the electronic properties of the molecules on the surface we have performed scanning tunnelling spectroscopy (STS) measurements. The results are compared with theoretically calculated transmission coefficient T(E) spectra. Figure 7 shows the state interaction diagram for the tribiphenylene **2a** with the analysis of the HOMO and LUMO orbitals of the molecule interacting with the π and π* orbitals of the DB dimer during the [4+2] Diels-Alder cycloaddition. The initially buckled DB dimer is characterized by a π–π* gap of approximately 1.8 eV (see most left column of Figure 7). When the DB dimer unbuckles to the configuration required for the [4+2] reaction, the states shift and the gap is decreased to 0.3 eV. We calculated the HOMO–LUMO gap for the flat molecule to be approximately 3.0 eV, as can be seen in the right column of Figure 7, and the same value is also obtained for the molecule physisorbed on a Ge(001):H surface without DBs. When the molecule is deformed to the final, bent configuration, the gap is reduced by 0.8 eV to approximately 2.2 eV, as indicated in the column "Deformed molecule" in Figure 7. We did not observe any significant changes in the energies of the orbitals HOMOb and LUMOb, but those of the orbitals HOMOa and LUMOa are altered significantly upon deformation. When the covalent bonds between the deformed molecule and the unbuckled DB dimer are created, the HOMOa and LUMOa orbitals of the tribiphenylene overlap with π and π* states of the DB dimer forming π-LUMO bonding state, located around 0.6 eV, and π*-HOMO at around 1.0 eV below the Fermi level, respectively. The π-LUMO bonding state has an important molecular contribution to the calculated transmission coefficient spectrum T(E), which displays a resonance at around 0.6 eV below Fermi level (Figure 8b, blue curve), very

close to the edge of the substrate valence band. The experimental filled state STM images of the tribiphenylene molecule attached to the DB dimer shown in Figure 3 are dominated by the contribution of this π-LUMO bonding state. The second T(E) resonance, which in the calculations is characterized by a lower intensity, appears around –1.0 eV, i.e., 0.1 eV lower in energy than the HOMO of the flat molecule as indicated in Figure 8b. This resonance comes from the second bonding state formed by overlapping HOMOa with the π* state of the DB dimer with an additional shoulder originating from the almost unchanged HOMOb orbital.

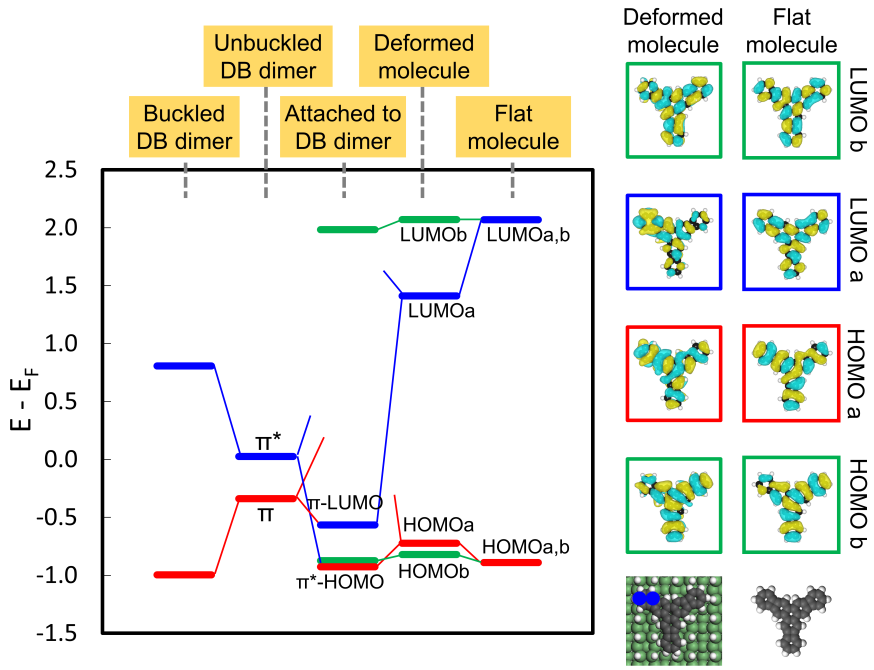

Figure 7. State interaction diagram calculated for tribiphenylene **2a** attached to the DB dimer; the left column shows the molecular orbital energy diagram, the right column presents calculated extended Hückel molecular orbitals (EHMO) of the molecule deformed to the attachment configuration (left) and the flat molecule (right); for the attached to the DB dimer configuration, the antibonding π*-HOMO and π-LUMO states are not shown, since they exhibit a large dispersion in the band structure and seemingly do not appear in the projected density of states (PDOS) and T(E).

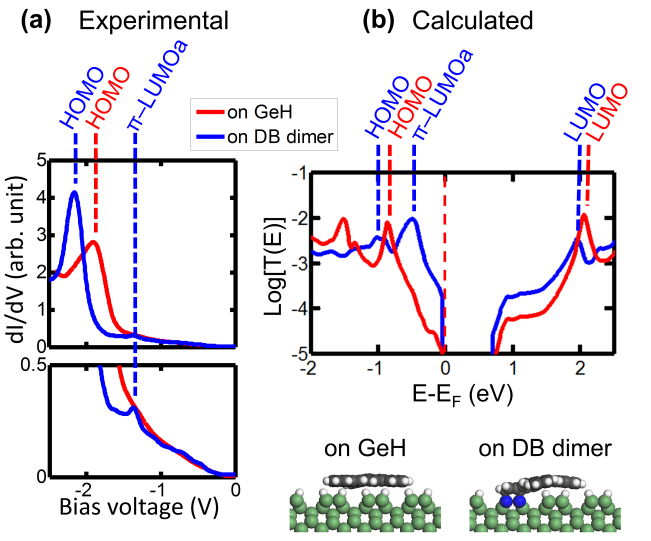

Figure 8. Comparison of experimental filled state STS data (a) and calculated transmission coefficient T(E) spectra (b) recorded over a tribiphenylene **2a** molecule physisorbed on a Ge(001):H surface (red) and covalently attached to the surface DB dimer (blue).

The positive voltage part of T(E) does not exhibit any resonance for moderate voltages. A prominent peak in the T(E) spectrum appears only at high voltages, around +2.0 eV, and corresponds to the LUMOb orbital. Due to the propensity of the molecules attached to the DB dimer for electron injection, we limited the analysis of the STS experiments to the filled states.

With respect to the molecule physisorbed on a Ge(001):H surface, with a relatively planar configuration as described in Section 6 of the ESI† (Figure S15), the recorded experimental spectrum (drawn in red in Figure 8a) is characterized by a flat part corresponding to the band gap and a prominent resonance centred at around –1.91 eV, which we attribute to the degenerate HOMO states of the molecule. This assumption is further supported by the good agreement between the experimental STM topography and the calculated appearance including the HOMO states, which are shown in ESI† (Figure S15). The curve recorded for the molecule attached covalently to the DB dimer (displayed in blue) displays a prominent resonance at around –2.17 V, slightly lower than the HOMO of the physisorbed molecule shown in red. This peak is attributed to the π*-HOMO state with the contribution of the HOMOb

state. The observed energetic shift with respect to the HOMO resonance of the physisorbed molecule by approximately 0.25 eV is somewhat larger than in the calculations, where it only amounts to 0.1 eV (Figure 8b). The spectrum contains an additional resonance characterized by a relatively small intensity and centred at around –1.4 eV below the Fermi level. It is attributed to the bonding π-LUMO state, in good agreement with the T(E) spectrum. This assignment is further supported by the good match between the experimental and calculated STM topographies of the chemically attached molecule, which are shown in Figure 3. Although the resonance positions are well described in our theoretical treatment, we observe disagreement in the intensity of the peaks. This disagreement can be fully explained by the close proximity of molecular and DB levels to the valence band,[31] which makes the resonance intensity exponentially dependent on the peak position relative to the valence edge. Our computational treatment, ignoring e.g. the tip-induced field, cannot describe intensities in this delicate regime.

Similar STS results are also obtained for hexafluorotribiphenylene **2b** with the general energetic downshift of HOMO and LUMO orbitals reflected in the recorded filled state STS resonances (see Figures S22 and S27 in ESI†). The electronic properties of the molecules, which stay pinned on the DB dimer after bond breaking, are discussed in detail in Section 10 of the ESI†. Interestingly, the measurements show a rigid upward shift of the π* orbital energy of the DB dimer located underneath the molecule compared to the bare DB dimer, which reflects the influence of the molecule on the positions of Ge atoms forming the DB dimer and the dimer buckling (ESI†, Figure S23).

Finally, we found that the interaction between the tribiphenylene molecule, as well as its fluoro–substituted counterpart, with single, unpaired DBs is strikingly different compared to covalent attachment to DB dimers. In the case of single DBs, the molecules interact only by weak van der Waals forces, and their electronic structure is not impaired significantly by the presence of the atomic defect (ESI†, Figure S27), apart from a slight resonance shift that may arise from single electron charging of the single DB.

Methods

Synthesis. All reactions were performed under argon atmosphere. THF, Et_2O, CH_2Cl_2 and CH_3CN were purchased from Fluka (puriss., absolute, over molecular sieve) and used as received. Acetone was dried over molecular sieves. Et_3N and i-Pr_2NEt were distilled under argon from CaH_2. $Pd(PPh_3)_4$ was prepared following published procedures.[32] Other commercial reagents were purchased from Aldrich Chemical Co. or ABCR and were used without further purification. TLC was performed on Merck silica gel 60 F254; chromatograms were visualized with UV light (254 nm and 360 nm) and/or by treating with Hanessian reagent system followed by heating. Flash chromatography was performed on Merck silica gel 60 (ASTM 230–400 mesh). Reported melting points are uncorrected and were measured in a Büchi B-540 instrument. ^{1}H and ^{13}C-NMR spectra were recorded in Varian AMX 300, Varian AMX 400 or Bruker WM-500 spectrometers. LR and HR mass spectra were recorded using EI (70 eV) with a HP-5988A spectrometer and MALDI-TOF with a Bruker Autoflex spectrometer. Tribiphenylene **2a** was synthesized as previously reported.[24] Experimental details and characterization data for the synthesis of **2b** and **2c** are provided in the ESI†.

Calculation scheme. Calculations were performed using density functional theory (DFT) based on the SIESTA code.[33] The surface is represented by a Ge slab containing 5 layers. The top surface is covered by the Ge(001)-(2x1):H dimer reconstruction with hydrogen vacancies when needed. The bottom surface is unreconstructed and fully hydrogen passivated. We used periodic boundary conditions with a 3 x 6 supercell of the reconstructed sur-face. In total, our slabs contain 286 atoms. We employed the optB88-vdW functional to describe exchange and correlation,[34] a k-point sampling of 2 x 3 x 1 (largest along the dimer rows), a mesh-cut-off of 300 Ry for real-space integrations, and a double-z plus polarization (DZP) basis set, using an energy shift of 100 meV for determining the cut-off radii. Relaxations were performed until all forces were below 0.02 eV Å^{-1}, fixing only the lower passivating layer of hydrogen. Adsorption energies were corrected using the counterpoise method.[35] Guided by experiment and previous work,[19] the initial geometries were chosen to position the centre of the phenyl rings directly above the DB dimer, with the corresponding molecule arm forming an angle of 0, 60 and 90 degrees with respect to the dimer rows on the surface. Desorption paths were calculated by constraining the molecular centre-of-mass to successively lie further and further away from the dimer. This path was then refined using the Nudged Elastic Band method.[30]

The STM images and transmission spectra, T(E), of the optimized structures were calculated using the surface Green function matching (SGFM) method with extended Hückel molecular orbital (EHMO) Hamiltonian,[29] which considers the couplings between the tip, molecule, Ge(001):H surface, and the bulk Ge.[8a,16,17] The EHMO parameters were fitted to DFT band structures as described by Kolmer et al.[8a] The Fermi level was set to allow matching between the π and π* orbitals of the buckled bare DB dimer and experimentally recorded resonances.[7a,7b,8a] Note that the bias voltages used in the calculations are in general smaller than those used in the experiments because the tip-induced band bending is not accounted for in the SGFM method, as described previously.[10,16] The molecular orbitals of the flat and deformed molecules were likewise calculated using the EHMO Hamiltonian.

Sample preparation. All experiments were performed in a multi-chamber ultrahigh vacuum system equipped with a low temperature STM manufactured by Omicron Nano-technology GmbH. STM and STS measurements were executed at liquid helium temperature using electrochemically etched tungsten tips. Germanium samples were prepared by a standard procedure of argon ion bombardment and thermal annealing

at 770 °C. Hydrogen passivation was achieved with a home-built hydrogen cracker to pro-vide a flux of hydrogen atoms to the surface.[8a] The molecules were thermally evaporated from a powder placed inside a Knudsen cell. The sublimation temperature was 265°C for tribiphenylene **2a**, 275°C for **2b** and 310 °C for **2c** derivatives. STM images were processed using SPIP and WSxM software.[36]

Conclusions

We reveal that tribiphenylenes, large polycyclic arenes containing the biphenylene structural motif, undergo a completely site-selective Diels-Alder reaction with paired surface DBs on a hydrogen passivated Ge(001):H surface. The detailed analysis of this transformation by high resolution STM/STS characterization, advanced DFT modelling and STM image simulations concludes that it constitutes a fully reversible concerted [4+2] cycloaddition, in which the molecules play the role of the conjugated diene. The observed bonding configuration confirms the expected selectivity of the reaction, which can be understood considering the significant degree of bond localization induced by the presence of the antiaromatic cyclobutadiene rings in the polycyclic structure and the reactivity trends shown by other simpler phenylenes in [4+2] cycloadditions in solution. The change in attachment orientation of the tribiphenylene vs. trinaphthylene topology provides a striking example of the application of simple molecular design principles to control the bonding configuration of polycyclic conjugated molecules on a surface. We also demonstrate that substituted derivatives show similar reactivity and the same site-selectivity as the parent tribiphenylene and that the barriers for attachment correlate with the shifts of the frontier orbital energy. Finally, STM tip-induced bond breaking enables the controlled switch from covalent attachment to the DB dimer to physisorption.

Detailed STS measurements of tribiphenylenes confirm the influence of electronic structure on the bonding to surface DB dimers. Our experiments corroborate also the theoretically calculated downward energy shift of the HOMO orbital of fluorinated derivatives compared to the parent tribiphenylene.

To sum up, we have demonstrated the feasibility of building up atomically precise structures by functionalization of semiconductor surfaces with large polycyclic conjugated molecules, by combining DBs patterning and molecular design. Work is in progress to extend this strategy to build complex circuits and devices.

Conflicts of interest

There are no conflicts to declare.

Acknowledgements

This work was supported by the FP7 FET-ICT ''Planar Atomic and Molecular Scale devices'' (PAMS) project (funded by the European Commission under contract no. 610446), by the Polish Ministry for Science and Higher Education from financial resources for science in 2013-2017 granted for an international co-financed project (contract no. 2913/7.PR/2013/2) and by projects CTQ2016-78157-R, MAT2016-78293-C6-3R and MAT2016-78293-C6-4R (AEI/FEDER, UE). EG, DP and DP are grateful for financial support from the Xunta de Galicia (Centro singular de investigación de Galicia accreditation 2016–2019, ED431G/09) and the European Union (European Regional Development Fund-ERDF). The STM experiments were carried out using equipment purchased with funding from the European Regional Development Fund within the framework of the Polish Innovation Economy Operational Program (contract no. POIG.02.01.00–12-023/08). MK acknowledges financial backing from the Foundation for Polish Science (FNP). HK is indebted to the A*STAR Computational Resource Centre (A*CRC) for computational resources and backing. RZ appreciates the support received from KNOW (scholarship KNOW/59/SS/RZ/2016). The authors thank Manuel Vilas (CIQUS) for the cyclic voltammetry data for **2a** and **2c**, and Berta Álvarez (CIQUS) for experiments exploring the reactivity of **2a** in solution, not included in this article.

Notes and references

(1) (a) W. G. Schmidt, K. Seino, M. Preuss, A. Hermann, F. Ortmann and F. Bechstedt, *Appl. Phys. A.*, 2006, **85**, 387–397.

(2) (a) N. Pavlicek and L. Gross, *Nature Rev.*, 2017, **1**, 0005. (b) L. Gross, F. Mohn, N. Moll, P. Liljeroth and G. Meyer, *Science*, 2009, **325**, 1110–1114. (c) L. Gross, F. Mohn, N. Moll, G. Meyer, R. Ebel, W. M. Abdel-Mageed and M. Jaspars, *Nature Chem.*, 2010, **2**, 821–825. (d) L. Gross, F. Mohn, N. Moll, B. Schuler, A. Criado, E. Guitián, D. Peña, A. Gourdon and G. Meyer, *Science*, 2012, **337**, 1326–1329. (e) D. G. De Oteyza, P. Gorman, Y.–C. Chen, S. Wickenburg, A. Riss, A. J. Mowbray, G. Etkin, Z. Pedramrazi, H.-Z. Tsai, A. Rubio, M. F. Crommie and F. R. Fischer, *Science*, 2013, **340**, 1434. (f) N. Pavlicek, B. Schuler, S. Collazos, N. Moll, D Pérez, E. Guitián, G. Meyer, D. Peña and L. Gross, *Nature Chem.*, 2015, **7**, 623–628. (g) A. Riss, A. Pérez Paz, S. Wickenburg, H.-Z. Tsai, D. G. De Oteyza, A. J. Bradley, M. M. Ugeda, P. Gorman, H. S. Jung, M. F. Crommie, A. Rubio and F. R. Fischer, *Nature Chem.*, 2016, **8**, 678.

(3) (a) R. Hoffmann, *Angew. Chem. Int. Ed.* 2013, **52**, 93-103. (b) For a recent, excellent illustration of this concept, see: L. Pecher, S. Leref, M. Raupach and R. Tonner, *Angew. Chem. Int. Ed.* 2017, **56**, DOI: 10.1002/anie.201707428.

(4) (a) R. J. Hamers, S. H. Coulter, M. D. Ellison, J. S. Hovis, D. F. Padowitz and M. P. Schwartz, *Acc. Chem. Res.*, 2000, **33**, 617–624. (b) H. N. Waltenburg and J. T. Yates, *Chem. Rev.*, 1995, **95**, 1589–1673.

(5) (a) F. Tao and S. L. Bernasek, (Eds.), *Functionalization of Semiconductor Surfaces*, John Wiley and Sons, Hoboken, NJ, USA, 2012. (b) T. R. Leftwich and A. V. Teplyakov, *Surf. Sci. Rep.*, 2008, **63**, 1–71. (c) D. Riedel, M.-L. Bocquet, H. Lesnard, M. Lastapis, N. Lorente, P. Sonnet and G. Dujardin, *J. Am. Chem. Soc.*, 2009, **131**, 7344–7352. (d) M. A. Filler and S. F. Bent, *Progr. Surf. Sci.*, 2003, **73**, 1–56. (e) P. W. Loscutoff and S. F. Bent, *Annu. Rev. Phys. Chem.*, 2006, **57**, 467–495.

(6) (a) K. R. Harikumar, J. C. Polanyi, A. Zhabet-Khosousi, P. Czekala, H. Lin and W. A. Hofer, *Nature Chem.*, 2011, **3**, 400–408. (b) Y. Wang and G. S. Hwang, *J. Chem. Phys.*, 2005, **122**, 164706.

(7) (a) M. Engelund, S. Godlewski, M. Kolmer, R. Zuzak, B. Such, T. Frederiksen, M. Szymonski and D. Sanchez-Portal, *Phys. Chem.*

Chem. Phys., 2016, **18**, 19309. (b) S. Godlewski, M. Kolmer, J. Lis, R. Zuzak, B. Such, W. Gren, M. Szymonski and L. Kantorovich, *Phys. Rev. B*, 2015, **92**, 115403; (c) M. Taucer, L. Livadaru, P. G. Piva, R. Achal, H. Labidi, J. L. Pitters and R. A. Wolkow, *Phys. Rev. Lett.*, 2014, **112**, 256801. (d) M. Baseer Haider, J. Pitters, G. DiLabio, L. Livadaru, J. Mutus and R. A. Wolkow, *Phys. Rev. Lett.*, 2009, **102**, 046805. (e) S. R. Schofield, P. Studer, C. F. Hirjibehedin, N. J. Curson, G. Aeppli, D. R. Bowler, *Nature Commun.* 2013, **4**, 1649; A. Bellec, L. Chaput, G. Dujardin, D. Riedel, L. Stauffer and P. Sonnet, *Phys. Rev. B: Condens. Matter Mater. Phys.*, 2013, **88**, 241406(R).

(8) (a) M. Kolmer, S. Godlewski, H. Kawai, B. Such, F. Krok, M. Saeys, C. Joachim and M. Szymonski, *Phys. Rev. B: Condens. Matter Mater. Phys.*, 2012, **86**, 125307. (b) M. Engelund, R. Zuzak, S. Godlewski, M. Kolmer, T. Frederiksen, A. Garcia-Lekue, D. Sanchez-Portal and M. Szymonski, *Sci. Rep.*, 2015, **5**, 14496. (c) M. Kolmer, R. Zuzak, G. Dridi, S. Godlewski, C. Joachim and M. Szymonski, *Nanoscale*, 2015, **7**, 12325–12330. (d) M. Fuechsle, S. Mahapatra, F. A. Zwanenburg, M. Friesen, M. A. Eriksson and M. Y. Simmons, *Nature Nanotechnol.*, 2010, **5**, 502–505. (e) B. Weber, S. Mahapatra, H. Ryu, S. Lee, A. Fuhrer, T. C. G. Reusch, D. L. Thompson, W. C. T. Lee, G. Klimeck, L. C. L. Hollenberg and M. Y. Simmons, *Science*, 2012, **335**, 64–67. (f) F. Bianco, D. R. Bowler, J. H. G. Owen, S. A. Köster, M. Longobardi and C. Renner, *ACS Nano*, 2013, **7**, 4422–4428.

(9) (a) P. G. Piva, G. A. DiLabio, J. L. Pitters, J. Zikovsky, M. Rezeq, S. Dogel, W. A. Hofer and R. A. Wolkow, *Nature*, 2005, **435**, 658–661. (b) Md. Z. Hossain, H. S. Kato and M. Kawai, *Phys. Chem B*, 2005, **109**, 23129–23133.

(10) S. Godlewski, M. Kolmer, M. Engelund, H. Kawai, R. Zuzak, A. Garcia-Lekue, M. Saeys, A. M. Echavarren, C. Joachim, D. Sanchez-Portal and M. Szymonski, *Phys. Chem. Chem. Phys.*, 2016, **18**, 3854–3861.

(11) P. M. Ryan, L. Livadaru, G. A. DiLabio and R. A. Wolkow, *J. Am. Chem. Soc.*, 2012, **134**, 12054–12063.

(12) (a) See ref. 5a, chapter 4: K. T. Wong and S. F. Bent, Pericyclic reactions of organic molecules at semiconductor surfaces, pp 51–88. (b) F. Tao and Q. C. Xu, *Acc. Chem. Res.*, 2004, **37**, 882–893. (c) M. P. Schwartz, M. D. Ellison, S. K. Coulter, J. S. Hovis and R. Hamers, *J. Am. Chem. Soc.*, 2000, **122**, 8529–853. (d) R. Konecny and D. J. Doren, *J. Am. Chem. Soc.*, 1997, **119**, 11098–11099. (e) A. V. Teplyakov, M. J. Kong and S. F. Bent, *J. Am. Chem. Soc.*, 1997, **119**, 11100–11101.

(13) (a) J. Baik, M. Kim, C.-Y. Park, C. Kim, J. R. Ahn and K.-S. An, *J. Am. Chem. Soc.*, 2006, **128**, 8370–8371. (b) X. Lu, X. Wang, Q. Yuan and G. Zhang, *J. Am. Chem. Soc.*, 2003, **125**, 7923–7929.

(14) F. Tao, S. L. Bernasek and G.-Q. Xu, *Chem. Rev.*, 2009, **109**, 3991–4024.

(15) See ref. 5a, chapter 7: K. S. Yong and G.-Q. Xu, Covalent Binding of Polycyclic Aromatic Hydrocarbon Systems, pp 163–191.

(16) S. Godlewski, M. Kolmer, H. Kawai, B. Such, R. Zuzak, M. Saeys, P. De Mendoza, A. M. Echavarren, C. Joachim and M. Szymonski, *ACS Nano*, 2013, **7**, 10105–10111.

(17) S. Godlewski, H. Kawai, M. Kolmer, R. Zuzak, A. M. Echavarren, C. Joachim, M. Szymonski and M. Sayes, *ACS Nano*, 2016, **10**, 8499–8507.

(18) W.-H. Soe, C. Manzano, N. Renaud, P. De Mendoza, A. De Sarkar, F. Ample, M. Hliwa, A. M. Echavarren, N. Chandrasekhar and C. Joachim, *ACS Nano*, 2011, **5**, 1436–1440.

(19) S. Godlewski, H. Kawai, M. Engelund, M. Kolmer, R. Zuzak, A. Garcia-Lekue, G. Novell-Leruth, A. M. Echavarren, D. Sanchez-Portal, C. Joachim and M. Saeys, *Phys. Chem. Chem. Phys.*, 2016, **18**, 16757–16765.

(20) K. P. C. Vollhardt and D. M. Mohler, *Advances in Strain in Or-ganic Chemistry*, Halton, B. Ed., JAI Press: London, 1996, pp 121–160.

(21) (a) O. Š. Miljanić and K. P. C. Vollhardt, *Carbon-Rich Compounds: From Molecules to Materials*, M. M. Haley and R. R. Tykwinski (Eds.); Wiley-VCH, Weinheim, 2006; pp 140−197. (b) The radialene structure of a biphenylene derivative has been studied recently at the molecular level by high-resolution AFM: S. Kawai, K. Takahashi, S. Ito, R. Pawlak, T. Meier, P. Spijker, F. Federici Canova, J. Tracey, K. Nozaki, A. S. Foster and E. Meyer, *ACS Nano*, 2017, **11**, 8122-8130.

(22) (a) L. Blanco, H. E. Helson, M. Hirthammer, H. Mestdagh, S. Spyroudis and K. P. C. Vollhardt, *Angew. Chem., Int. Ed. Engl.*, 1987, **26**, 1246–1247. (b) R. H. Schmidt-Radde and K. P. C. Vollhardt, *J. Am. Chem. Soc.*, 1992, **114**, 9713–9715. (c) C. Eickmeier, D. Holmes, H. Junga, A. J. Matzger, F. Scherhag, M. Shim and K. P. C. Vollhardt, *Angew. Chem., Int. Ed.*, 1999, **38**, 800–804. (d) R. Boese, A. J. Matzger, D. L. Mohler and K. P. C. Vollhardt, *Angew. Chem., Int. Ed. Engl.*, 1995, **34**, 1478–1481. (e) S. Han, D. R. Anderson, A. D. Bond, H. V. Chu, R. L. Disch, D. Holmes, J. M. Schulman, S. J. Teat, K. P. C. Vollhardt and G. D. Whitener, *Angew. Chem. Int. Ed.*, 2002, **41**, 3227–3230.

(23) (a) R. R. Parkhurst and T. M. Swager, *J. Am. Chem. Soc.*, 2012, **134**, 15351−15356. (b) Z. Jin, Y. C. Teo, N. G. Zulaybar, M. D. Smith, Y. Xia, *J. Am. Chem. Soc.*, 2017, **139**, 1806–1809.

(24) B. Iglesias, A. Cobas, D. Pérez and E. Guitián, *Org. Lett.*, 2004, **6**, 3557–3560.

(25) (a) F. Schlütter, T. Nishiuchi, V. Enkelmann, K. Müllen, *Angew. Chem. Int. Ed.*, 2014, **53**, 1538 –1542. (b) Q. Song, B. Wang, K. Deng, X. Feng, M. Wagner, J. G. Gale, K. Müllen, L. J. Zhi, *Mater. Chem. C*, 2013, **1**, 38–41. (c) S. Wang, *Materials Lett.*, 2016, **167**, 258–261. (d) M. Liu, M. Liu, L. She, Z. Zha, J. Pan, S. Li, T. Li, Y. He, Z. Cai, J. Wang, Y. Zheng, X. Qiu and D. Zhong *Nature Commun.* 2017, **8**, 14924.

(26) P. Bao and Z.-H. Yu, *J. Phys. Org. Chem.*, 2010, **23**, 16–29.

(27) See ESI† for the synthesis and characterization details of **2b** and **2c**.

(28) There are two examples of [4+2] cycloadditions to biphenylene in solution, featuring 2,4a-cycloadducts (in contrast to the 1,4-selectivity shown by naphthalene): (a) H. Heaney, K. G. Mason and J. M. Sketchley, *Tetrahedron Lett.*, 1970, **11**, 485–488. (b) W. Adam and M. Balci, H. J. Kiliç, *Org. Chem.*, 1998, **63**, 8544–46. For [4+2] cycloadditions of other phenylenes, see: (c) H. Mestdagh and K. P. C. Vollhardt, *J. Chem. Soc., Chem. Commun.*, 1986, 281–282. (d) S. Kumaraswamy, S. S. Jalisatgi, A. J. Matzger, O. S. Miljanic and K. P. C. Vollhardt, *Angew. Chem. Int. Ed.*, 2004, **43**, 3711–3715.

(29) J. Cerdá, M. S. Van Hove, P. Sautet and M. Salmeron, *Phys. Rev. B*, 1997, **56**, 15885.

(30) (a) H. Jónsson, G. Mills and K. W. Jacobsen, Nudged Elastic Band Method for Finding Minimum Energy Paths of Transitions, in Classical and Quantum Dynamics in Condensed Phase Simulations, B. J. Berne, G. Ciccotti, G. and D. F. Coker (Eds.), World Scientific, 1998. (b) G. Henkelman, B. P. Uberuaga and H. Jónsson, *J. Chem. Phys.*, 2000, **113**, 9901–9904.

(31) M. Wojtaszek, R. Zuzak, S. Godlewski, M. Kolmer, J. Lis and M. Szymonski, *J. Appl. Phys.*, 2015, **118**, 185703.

(32) L. S. Hegedus, *Palladium in Organic Synthesis in Organometallics in Synthesis: A Manual*, Schlosser, M. (Ed.), John Wiley and Sons, New York, 1994.

(33) (a) J. M. Soler, E. Artacho, J. D. Gale, A. Garcia, J. Junquera, P. Ordejon and D. Sanchez-Portal, *J. Phys.: Condens. Matter*, 2002, **14**, 2745–2779. (b) D. Sanchez-Portal, P. Ordejon, E. Artacho and J. M. Soler, *Int. J. Quantum Chem.*, 1997, **61**, 453–461. (c) E. Artacho, D. Sanchez-Portal, P. Ordejon, A. Garcıa and J. M. Soler, *Phys. Status Solidi B*, 1999, **215**, 809–817.

(34) (a) M. Dion, H. Rydberg, E. Schroeder, D. C. Langreth and B. I., Lundqvist, *Phys. Rev. Lett.*, 2004, **92**, 246401. (b) J. Klimeš, D. R. Bowler and A. Michaelides, *Phys. Rev. B*, 2011, **83**, 195131.

(35) S. F. Boys and F. Bernardi, *Mol. Phys.*, 1970, **19**, 553–566.

(36) I. Horcas, R. Fernandez, J. M. Gomez-Rodriguez, J. Colchero, J. Gomez-Herrero and A. M. Baro, *Rev. Sci. Instrum.*, 2007, **78**, 013705.